Interplay between *A*-site and *B*-site driven instabilities in perovskites

M. Ghita and M. Fornari

Department of Physics, Central Michigan University, Mt. Pleasant, Michigan 48859, USA

D. J. Singh

Condensed Matter Sciences Division, Oak Ridge National Laboratory, Oak Ridge, Tennessee 37831, USA

S. V. Halilov

RJ Mears LLC, 1100 Winter St., Waltham, Massachusetts 02451, USA

Density functional calculations are used to investigate the trends in the lattice instabilities of the perovskites, $BaTiO_3$, $PbTiO_3$, $BaZrO_3$, and $PbZrO_3$ with volume. A simple scheme for classifying perovskites in terms of *A*-site and *B*-site activities is discussed in relation to competition between rhombohedral and tetragonal ground states.

PACS number(s): 77.84.Dy, 71.15.Nc

I. INTRODUCTION

Perovskite solid solutions provide most of the technologically useful ferroelectric and piezoelectric materials, including $Pb(Zr, Ti)O_3$ (PZT), which is the dominant electro active material in applications.[1–3] As such, these materials have been extensively studied and much is understood about them. For example, detailed investigations of the PZT phase diagram have revealed the presence of a monoclinic bridging phase at the so-called morphotropic phase boundary (MPB) between the rhombohedral (R) and tetragonal (T) ferroelectric phases, which plays a key role in the piezoelectric performance of the material.[4–6] The structure and position of this boundary and other details of the PZT phase diagram have been well reproduced by first principles based calculations.[7] While important insights have been gained in recent years, the microscopic understanding needed to chemically control the existence and position of MPBs has yet to be established.

To discuss the lattice instabilities of insulating perovskites ABO_3 it is useful to divide them into two groups based on the tolerance factor, $t = (r_O + r_A)/\sqrt{2}(r_O + r_B)$, where r_O, r_A and r_B are the ionic radii[8,9] of the O, *A*, and *B* ions. Perovskites with $t > 1$ including the classical ferroelectric systems, like $BaTiO_3$, are called *B*-site driven, because the *B*-site cation (i.e., Ti) is nominally too small for its site, and may tend to displace. These materials are typically ferroelectric with rhombohedral or similar structures that have small lattice strain. They do not show MPB's that are useful for piezoelectric application. Conversely, $t < 1$ or so-called *A*-site driven materials are generally not ferroelectric at all, and instead find favorable bond lengths by tilts and rotations of the BO_6 octahedra yielding structures like the prototypical $GdFeO_3$ (*Pnma*) structure. The notable exceptions are materials with Pb^{2+} as the *A*-site cation, as in PZT, in which case *A*-site driven ferroelectricity occurs along with piezoelectrically active MPB's. The role of Pb in these materials has long been understood in terms of the Pb^{2+} electronic structure, which has a relatively large high-lying occupied 6*s* orbital and a relatively low-lying, extended, unoccupied 6*p*

state. This is discussed in terms of the so-called "polarizable lone pair" of Pb^{2+}, but actually is due to cross gap hybridization between occupied O 2*p* states and unoccupied Pb 6*p* states, similar to the cross-gap *B*-site—O hybridization that generally favors ferroelectricity in oxides.[10]

This understanding has focused efforts at finding new piezoelectrics on Pb containing perovskites and some closely related chemistries, like Bi. However, recent studies of different *A*-site substitutions yielded interesting results, such as the increase in tetragonality when alloying with small *A*-site ions.[11–14] More significantly, Saito and coworkers recently reported a textured $(Li, Na, K)(Nb, Ta, Sb)O_3$ perovskite material that has piezoelectric performance similar to ceramic PZT.[15] The purpose of the present work is to use density functional calculations of the volume dependence of lattice instabilities of several perovskites from different classes to elucidate trends in the interplay of *A*-site and *B*-site driven instabilities in this class of materials. Density functional calculations are particularly useful for this because they allow calculations using structural symmetry constraints. So for example, one can study the tetragonal ferroelectric, rhombohedral ferroelectric, and octahedrally rotated structures independently even though they may not correspond to the experimentally accessible ground state.

II. DENSITY FUNCTIONAL APPROACH

Here we investigate four compounds: $BaTiO_3$ (BT), $PbTiO_3$ (PT), $PbZrO_3$ (PZ), and $BaZrO_3$ (BZ) as well as a fcc ordered supercell of PZT with composition $PbZr_{0.5}Ti_{0.5}O_3$. This chemical variation plus the strong volume dependence often found in perovskite lattice instabilities, including PZT is used here.[16–18] The calculations were done using the local density approximation (LDA) with ultra-soft pseudopotentials[19] as implemented in the PWSCF code.[20] A large plane wave cutoff of 30 Ry and (6,6,6) or equivalent grids for *k*-space sampling were used to ensure the convergence in all the calculations presented here. The energetic and the structural parameters (Tables I and II are in good agreement with previous results.[10,21–26]

TABLE I. Calculated total energies of BT, PZ, PT, and PZT with various symmetry constrained lattice distortions done at the experimental volume. The energies are in millirydbergs per formula unit and are relative to the ideal cubic perovskite structure. The distortions are R (rhombohedral ferroelectric), T_0 (tetragonal ferroelectric, with no strain, $c/a=0$), T (tetragonal ferroelectric—the calculated value of c/a follows), and ROT111 (octahedral rotation around 111).

	R	T_0	T	c/a	ROT111
BT	−3.2	−1.6	−2.8	1.037	0.0
PZ	−20.1	−14.5	−16.1	1.035	−16.9
PT	−10.0	−9.8	−14.9	1.102	−0.2
PZT	−12.9	−10.3	−12.6	1.054	−3.9

III. ROLE OF *A*- AND *B*-SITE CATIONS

One of the key ingredients in understanding the occurrence of MPB's in *A*-site driven ferroelectric perovskites is identifying the mechanisms that stabilize the rhombohedral phase. Specifically, in the perovskite structure the *A* ion is on a cubic site, with a 12-fold nearest neighbor oxygen environment. This is a highly isotropic environment, and so it may be expected that the energetics associated with *A*-site off centering would also be highly isotropic. The ferroelectric mode couples to strain for tetragonal (T) off centering, but couples very weakly to strain for rhombohedral (R) off centering.[27,28] Therefore one would anticipate T ground states for strongly *A*-site driven ferroelectric perovskites. This is at odds with what is known about the PZT phase diagram, where a lower tolerance factor, Zr rich region is rhombohedral and the higher tolerance factor, Ti rich region is tetragonal.

We begin with the primitive five-atom cells of BT, BZ, PT, and PZ where we independently off center the *A*- and *B*-site cations with respect to the other ions, in other words supressing the intersublattice cooperation that is present in

TABLE II. Atomic displacements in a_B relative to the O center of mass for the symmetry constrained rhombohedral ferroelectric structures. The *A*-site and *B*-site displacements are (A_x,A_x,A_x) and (B_x,B_x,B_x), while the O displacements are (O_x,O_x,O_z) and permutations. r denotes the ratio A_x/B_x. BT (exp) denotes experimental results at 15 K from Ref. 36. Calculations are at the experimental volume V_{expt} and a 6% expanded volume $V_{stretch}$.

	A_x	B_x	O_x	O_z	r
V_{expt}					
BT	0.095	0.211	0.021	−0.042	0.45
BT(exp)	0.104	0.200	0.021	−0.042	0.52
PT	0.479	0.295	−0.015	0.029	1.63
PZ	0.643	0.281	−0.077	0.153	2.29
$V_{stretch}$					
BT	0.183	0.296	0.039	−0.078	0.62
PT	0.597	0.372	−0.003	0.006	1.60
PZ	0.749	0.294	−0.069	0.138	2.55
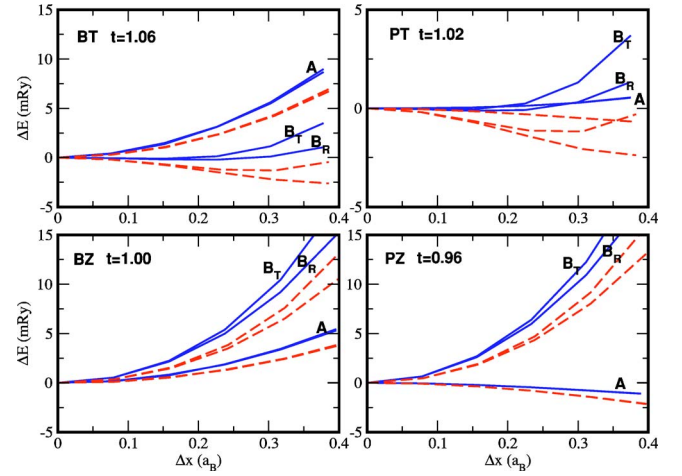
FIG. 1. (Color online) Energy dependence of the displacement of cation sublattices. The calculations are done displacing the *A* or *B* site cations along the tetragonal (T) and the rhombohedral (R) directions. The energy of the prototype cubic phase determines the zero. The curve corresponding to the *A* site off centering is isotropic (R and T displacement overlap) and is labeled (A). B_R and B_T identify the off-centering of the *B* site in the R and T directions, respectively. The solid line denotes the experimental volume, the dashed line show the effect of a 6% expansion.

the ferroelectric modes in perovskites. These calculations were done at the experimental volume and for a 6% volume expansion and displacements along [111] and [001], while keeping the lattice vectors fixed. As shown in Fig. 1, the four materials represent the four possible classes of behavior for single sublattice off centering; we denote these S, or stable against motion of either sublattice, represented by BZ, U_A, unstable against *A*-site off centering, represented by PZ, U_B, unstable against *B*-site off centering, represented by BT, and U_{AB}, unstable against both *A*- and *B*-sites off-centering, represented by PT. Materials in class U_B are *B*-site driven, $t>1$ ferroelectrics. Class S includes both stable cubic perovskites, like BZ, with $t\sim 1$, and ferroelectric materials like $KNbO_3$, which has $t>1$, and therefore may be classified as *B*-site driven, but where the ferroelectric instability only exists when the *A*- and *B*-site ions can move in a cooperative way.[29,30] Class U_B also contains *B*-site driven ferroelectrics, with $t>1$, while one may anticipate that class U_A materials are usually not ferroelectric due to octahedral rotation in these *A*-site driven $t<1$ materials, though this class also includes PZT and other *A*-site driven ferroelectrics. $PbTiO_3$, which has $t\sim 1$, belongs to the final class U_{AB}. Its tolerance factor is slightly larger than $SrTiO_3$, which favors weak *B*-site driven instabilities, but it also has an important contribution from Pb—O covalency as discussed by Cohen,[10] which favors Pb off centering.

All four materials are practically isotropic for *A*-site displacement, both at their experimental volumes and at expanded volumes, where the off-centering displacements are softer. This is equally true for the Ba containing compounds as for the Pb compounds, regardless of the fact that Pb—O hybridization is important for stabilizing *A*-site driven ferroelectricity, and regardless of the tolerance factor of the material. On the other hand, the displacement of the *B*-site ion is

noticeably anisotropic, and in all materials the rhombohedral direction is favored. Thus rhombohedral ground states are favored by the *B*-site displacement and this is what competes against the strain coupling, which as mentioned favors tetragonal ground states. Both of these effects make contributions to the total energy in fourth order in the ferroelectric mode amplitude and so the competition between them can be effective both for materials with large ferroelectric atomic displacements as well as materials with small displacements. The fact that the tendency toward rhombohedral ground states is driven entirely by the *B* site is no doubt at the root of the observation that in materials with large cation displacements the *B*-site and *A*-site displacements may be noncollinear, with *B*-site displacements along directions near [111].[31–34]

The ferroelectric modes in perovskites are generally cooperative. In other words, even though the tolerance factor is quite predictive in regard to what pattern of instability will occur in a given material, the simple notion that ferroelectricity consists of an off centering of the cation with the most space available is not strictly correct. This is evident from the known ground state structures of the materials. This is the case even in materials such as $BaTiO_3$, which has a large $t \sim 1.06$, and a simple alkaline earth *A*-site ion, but still has a substantial Ba off centering cooperating with the Ti motion.[35,36] The driving force for this includes electrostatic interactions and, in the case of Pb, bond competition, as discussed by Grinberg and coworkers[32,33] and Grinberg and Rappe.[34] The reason why good ferroelectrics have this tendency can be understood in terms of the Clausius-Mossotti relation, which reflects the fact that high polarizability per unit volume favors ferroelectricity over other competing non-ferroelectric lattice instabilities. Thus besides contributing to the polarization, cooperative off centering of both sites favors ferroelectricity due to the contribution of the passive site to the polarizability. In *A*-site driven ferroelectrics, especially, the competing instabilities due to octahedral rotation are generally important,[9,17,18] so this cooperation between the two cation sublattices can select between a ferroelectric and a nonferroelectric ground state.

Table II gives the relaxed symmetry constrained rhombohedral ferroelectric structure for BT, PT, and PZ, along with comparison to the experimental low temperature structure[36] for BT, which has a rhombohedral ferroelectric ground state. For $BaTiO_3$ the LDA ground state structure agrees well with experiment, as was found previously.[21] (LDA) calculations for the actual antiferroelectric orthorhombic structure of PZ have been shown to be in excellent agreement with recent neutron refinements of that structure.[23,24,37] For PT, there are significant LDA errors in the ground state structure, specifically the tetragonal c/a, related to a strong dependence of tetragonal strain on volume.[38] This issue is avoided here by doing calculations at fixed volume. BZ has no structural instability and is not shown. As shown, both cation species displace significantly with respect to the O center of mass in the ferroelectric structures. In BT, the ratio of the *A*-site to the *B*-site displacement is $r=0.45$ (LDA) and $r=0.52$ (experiment), i.e., less than unity as expected for a *B*-site driven ferroelectric. PZ has $r=2.29$ ($1/r=0.44$) reflecting its *A*-site driven ferroelectricity. The other difference between the
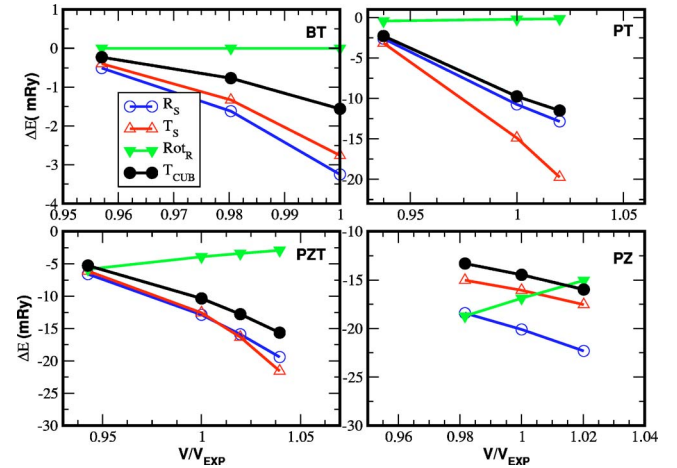
FIG. 2. (Color online) Energetics of the basic lattice instabilities as a function of volume, normalized to the experimental volume, for BT, PT, PZ, and the PZT supercell (see text). The energy is per perovskite unit cell (1/2 the supercell for PZT). The lattice instabilities shown are for the rhombohedral ferroelectric (R_s), tetragonal ferroelectric including tetragonal strain (T_s), tetragonal ferroelectric constrained to $c/a=1$ (T_{cub}) and centrosymmetric with octahedral rotation around [111] (Rot_r). Zero energy corresponds to the ideal cubic perovskite structure at the same volume. For BT the Rot_r curve is at zero for the entire volume range studied, corresponding to no rotational instability. Note the lower energy and volume scales for BT.

A-site driven and *B*-site driven materials is the distortion of the O octahedra. In BT, the displacement of the O transverse to the *B*-site—O bond is smaller than that along the bond (note that the O displacement is opposite to the cations), while in PZ transverse displacement is larger. This reflects the larger *A*-site displacement and the *A*-site O geometry. Based on these two considerations, PT is like PZ and not BT, and so should be regarded as strongly *A*-site driven, even though the nominal tolerance factor is slightly larger than unity. Compression suppresses ferroelectricity, while expansion increases the size of the ferroelectric instabilities. However, the character of the ferroelectricity as characterized by the ratio of cation displacements is little changed.

IV. VOLUME DEPENDENCE AND ROTATIONAL INSTABILITIES

Figure 2 gives the volume dependence of the basic lattice instabilities for BT, PT, and PZ as well as the PZT supercell. BZ (not shown) is stable in the ideal cubic perovskite structure. The rotational instability was calculated by relaxing doubled fcc 10 atom supercells cells (like the PZT supercell) with a centrosymmetric constraint. In BT there is no rotational instability in the volume range studied. In PT the rotational instability is induced by compression. In PZ and the PZT supercell there are substantial rotational instabilities at the experimental volume, and in both cases these become stronger as the volume is reduced. This is in contrast to the very weak volume dependence found previously in scandates.[14] This is an indication the ZrO_6 and TiO_6 octahe-

dra are stiff with respect to the Pb—O interactions. This is consistent with the linear response phonon dispersion curves of cubic perovskite PT and PZ,[39] which show strong upward dispersion of the R_{25} rotational instability when going away from the zone boundary, but weak dispersion of the unstable Γ_{25} ferroelectric instability across the zone. This means that the coherence length of a phase with rotational character would be necessarily longer that the A-site driven ferroelectric phase, and suggests that substitutions to produce A-site cation disorder would affect the rotational instabilities more strongly than the ferrolectric instabilities. This was found not to be an effective mechanism in the scandates with very weakly volume dependent rotational instabilities studied in Ref. 14. This means that the pressure dependence of the rotational instability, which is readily calculated for actual or notional materials, could be used to characterize the stiffness of the octahedra and the degree to which the rotational instability could be controlled by introducing A-site disorder. This pressure dependence can be also measured experimentally by inelastic neutron scattering (i.e., the R_{25} phonon frequency) if it is a stable mode, or structure refinement for a material with rotations. There have been experimental studies and model calculations of Sr and Ba doping in PZT ceramics, and for the case of Ba some shift of the MPB was indicated.[40,41]

Turning to the ferroelectric instabilities, Fig. 2 also shows the volume dependence of the symmetry constrained rhombohedral ferroelectric (R_s), tetragonal ferroelectric including tetragonal strain (T_s) and tetragonal ferroelectric constrained to $c/a=1$ (T_{cub}) instabilities. For BT, PT, PZ, and the PZT supercell the instability to the rhombohedral state is significantly stronger than T_{cub} over the whole volume range, and the magnitude of the energy difference between the two increases as the volume is increased. This increasing difference between the tetragonal and rhombohedral instabilities reflects the fact that, due to the cubic symmetry of the perovskite structure, the difference occurs at the next order in the amplitude of the distortion than the energy itself.

In PT the tetragonal strain is large and strongly stabilizes the tetragonal ferroelectric state over the volume range studied, but with greater stabilization at higher volume as expected. For PZT a somewhat lower stabilization is found, and since the difference between the unstrained tetragonal and rhombohedral states was larger to begin with, the effect of the strain is to make the tetragonal and rhombohedral states nearly degenerate as expected from the PZT phase diagram. In PZ, the strain energy is comparable to the PZT supercell and lower than in PT. It is insufficient to stabilize the tetragonal state, and the rhombohedral structure is strongly favored, again as expected from the known PZT phase diagram. The lower strain energy can be understood from the ionic radius. In particular, tetragonal deformation of the ZrO_6 octahedra is disfavored because it would require compression of the Zr—O bonds in this low tolerance factor perovskite. Turning to the PZT supercell, a comparison of the different instabilities as a function of volume is given in Table III. Previous calculations show that while the structural energy differences associated with B-site cation ordering are large compared to the ferroelectric energy,[25] the symmetric ordered supercell considered here does reproduce the ordering and energetics of the main ferroelectric phases in PZT at

TABLE III. Total energy of symmetry constrained ferroelectric distortions in PZT at different volumes. The values are in millirydbergs and the cubic perovskite structure at the same volume is used as a reference. R, T, M1, and M2 denote the rhombohedral, tetragonal, and monoclinic [(100) mirror], and monoclinic [(110) mirror], respectively.

V (a_B^3)	R	T	M1	M2
857.32	−13.16	−12.20	−12.73	
909.51	−25.75	−25.11	−25.46	
927.37	−31.76	−32.64	−32.78	−31.77
945.46	−38.82	−43.11	−43.18	−39.04

50% Zr.[17,25,26] Real PZT shows no evidence for B-site cation ordering, presumably because of the high temperature at which cations become immobile in the lattice. For our prototype supercell (space group, $Fm\overline{3}m$) two monoclinic distortions with Cm symmetry are possible depending on the orientation of the mirror plane [we used the label M1 for (100) and M2 for (110)]. At the theoretically determined volume ($V=857$ a_B^3) the calculated ground state is R (space group $R3m$). M2 and T (space group $I4mm$, including the supercell B-site cation ordering) are, however, less than 1 mRy higher in energy than the R phase. Expanding the system to the experimental volume ($V=910$ a_B^3) the R and T ferroelectric structures become degenerate to within the precision of the calculation, and with further expansion the lowest energy structure becomes T, as shown in Fig. 2, consistent with the experimental phase diagram of PZT, which has the MPB at $x=0.47$.[1] By comparison a crossing near the experimental volume does not occur in PT, PZ, or BT (Fig. 2). In fact, the volume dependence of the difference between the R and T energies is relatively weak in the PZT supercell compared to PT, but it is significant in PZT because of the near degeneracy of the R and T structures to start with.

V. CONCLUSIONS

In conclusion we have analyzed the volume dependence of the rotational and FE instabilities in several compounds. Our results show that anisotropic behavior is due to the B site regardless of whether or not the compound can be considered A-site active. The classification of ferroelectric perovskites in terms of A and B site motions provides a simple scheme to identify the ingredients of MPB systems and may be useful for adjusting the properties of perovskite MPB systems. For example, substitution of less covalent B-site ions (e.g., Ta for Nb) could be used to reduce the role of the B site and the tendency toward a rhombohedral ground state, if that was desired, and conversely greater B-site activity might be used to increase the size of the rhombohedral region of perovskite ferroelectric phase diagrams.

ACKNOWLEDGMENTS

[1] B. Jaffe, W. R. Cook, and H. Jaffe, *Piezoelectric Ceramics* (Academic Press, New York, 1971).

[2] K. Uchino, *Piezoelectric Actuators and Ultrasonic Motors* (Kluwer Academic, Boston, 1996).

[3] E. Cross, Nature (London) **432**, 24 (2004).

[4] B. Noheda, D. E. Cox, G. Shirane, L. E. Cross, and S. E. Park, Appl. Phys. Lett. **74**, 2059 (1999).

[5] R. Guo, L. E. Cross, S. E. Park, B. Noheda, D. E. Cox, and G. Shirane, Phys. Rev. Lett. **84**, 5423 (2000).

[6] H. Fu and R. E. Cohen, Nature (London) **403**, 281 (2000).

[7] L. Bellaiche, A. Garcia, and D. Vanderbilt, Phys. Rev. Lett. **84**, 5427 (2000).

[8] R. Shannon, Acta Crystallogr., Sect. A: Cryst. Phys., Diffr., Theor. Gen. Crystallogr. **32**, 751 (1976).

[9] W. Zhong and D. Vanderbilt, Phys. Rev. Lett. **74**, 2587 (1995).

[10] R. E. Cohen, Nature (London) **358**, 137 (1992).

[11] S. V. Halilov, M. Fornari, and D. J. Singh, Appl. Phys. Lett. **81**, 3443 (2002).

[12] D. Y. Suáres-Sandoval and P. K. Davies, Appl. Phys. Lett. **82**, 3215 (2003).

[13] I. Grinberg and A. M. Rappe, AIP Conf. Proc. **677**, 130 (2003).

[14] S. V. Halilov, M. Fornari, and D. J. Singh, Phys. Rev. B **69**, 174107 (2004).

[15] Y. Saito, H. Takao, T. Tani, T. Nonoyama, K. Takatori, T. Homma, T. Nagaya, and M. Nakamura, Nature (London) **432**, 84 (2004).

[16] G. A. Samara, Phys. Rev. B **1**, 3777 (1970).

[17] M. Fornari and D. J. Singh, Phys. Rev. B **63**, 092101 (2001).

[18] A. Sani, B. Noheda, I. A. Kornev, L. Bellaiche, P. Bouvier, and J. Kreisel, Phys. Rev. B **69**, 020105(R) (2004).

[19] D. Vanderbilt, Phys. Rev. B **41**, R7892 (1990).

[20] S. Baroni, A. Dal Corso, S. de Gironcoli, P. Giannozzi, C. Cavazzoni, G. Ballabio, S. Scandolo, G. Chiarotti, P. Focher, A. Pasquarello, K. Laasonen, A. Trave, R. Car, N. Marzari, and A. Kokalj, http://www.pwscf.org

[21] R. E. Cohen and H. Krakauer, Phys. Rev. B **42**, 6416 (1990).

[22] P. Ghosez, X. Gonze, and J. P. Michenaud, Ferroelectrics **220**, 1 (1999).

[23] D. J. Singh, Phys. Rev. B **52**, 12559 (1995).

[24] M. D. Johannes and D. J. Singh, Phys. Rev. B **71**, 212101 (2005).

[25] H. Fu and O. Gulseren, Phys. Rev. B **66**, 214114 (2002).

[26] Z. Wu and H. Krakauer, Phys. Rev. B **68**, 014112 (2003).

[27] W. Zhong, D. Vanderbilt, and K. M. Rabe, Phys. Rev. B **52**, 6301 (1995).

[28] T. Hashimoto, T. Nishimatsu, H. Mizuseki, Y. Kawazoe, A. Sasaki, and Y. Ikeda, Jpn. J. Appl. Phys., Part 2 **43**, 6785 (2004).

[29] D. J. Singh and L. L. Boyer, Ferroelectrics **136**, 95 (1992).

[30] D. J. Singh, Phys. Rev. B **53**, 176 (1996).

[31] W. Dmowski, M. K. Akbas, P. K. Davies, and T. Egami, J. Phys. Chem. Solids **61**, 229 (2000).

[32] I. Grinberg, V. R. Cooper, and A. M. Rappe, Nature (London) **419**, 909 (2002).

[33] I. Grinberg, V. R. Cooper, and A. M. Rappe, Phys. Rev. B **69**, 144118 (2004).

[34] I. Grinberg and A. M. Rappe, Phys. Rev. B **70**, 220101(R) (2004).

[35] A. W. Hewat, Ferroelectrics **6**, 215 (1974).

[36] G. H. Kwei, A. C. Lawson, S. J. L. Billinge, and S. W. Cheong, J. Phys. Chem. **97**, 2368 (1993).

[37] H. Fujishita, Y. Ishikawa, S. Tanaka, A. Ogawaguchi, and S. Katano, J. Phys. Soc. Jpn. **72**, 1426 (2003).

[38] Z. G. Wu, R. E. Cohen, and D. J. Singh, Phys. Rev. B **70**, 104112 (2004).

[39] P. Ghosez, E. Cockayne, U. V. Waghmare, and K. M. Rabe, Phys. Rev. B **60**, 836 (1999).

[40] R. S. Nasar, M. Cerqueira, E. Longo, E. R. Leite, J. A. Varela, A. Beltran, and J. Andres, J. Mater. Sci. **34**, 3659 (1999).

[41] R. S. Nasar, M. Cerqueira, E. Longo, J. A. Varela, and A. Beltran, J. Eur. Ceram. Soc. **22**, 209 (2002).